Statistical and event analysis of phase and amplitude scintillations associated with polar cap patches

Alanah Cardenas-O'Toole[1], Shasha Zou[1], Jiaen Ren[1], Jayachandran Thayyil[2]

[1]University of Michigan Department of Climate and Space Sciences and Engineering [2]University of New Brunswick

1) Introduction

- Ionospheric scintillation can degrade the GNSS signals and has the potential to cause a loss of access to GNSS services.
- Figure 1 shows a visual representation of the impacts of ionospheric structures on communication and navigation, including polar cap patches.
- Using a polar cap patch database provided by Ren et al. [2018] and scintillation data from 2016 provided by CHAIN, we study whether and how polar cap patches impact ionospheric scintillation.
- **It was found that ~80% patches do not lead to significant phase or amplitude scintillation increases in the polar cap, but occasionally they do lead to enhanced scintillations and preferentially near noon. We also found that the larger the patch density gradients, the higher the scintillation levels.**

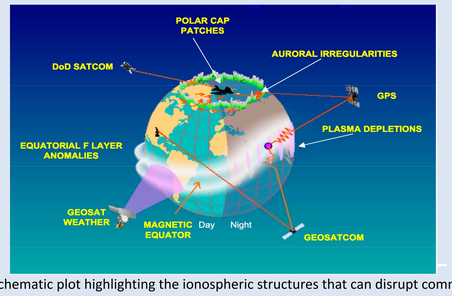

Figure 1. Schematic plot highlighting the ionospheric structures that can disrupt communication and navigation signals (From Basu, 2003). This proposal targets high-latitude irregularities and scintillations.

2) About the Data

- This study adapts a patch identifying algorithm from Ren et al. [2018] and applies to the RISR-C data in 2016. Density enhancements in the F-region of the ionosphere that had a density at least double the surrounding plasma [Crowley, 1996] and had halfwidths that lasted between 3 minutes and 2 hours are defined as patches. The time criterion was based on the typical patch size of 100 -1,000 km [Coley & Heelis, 1995] and the patch convection velocity ranging between 150 and 500 m/s [Hosokawa et al., 2009].
- We found 550 patches in 2016 and used 444 patches for this study with simultaneous scintillation measurements.
- The Canadian High Arctic Ionospheric Network (CHAIN) GPS receiver collocated with RISR-C provided the phase and amplitude scintillation data for the patches.
- In order to exclude multi-path effects and identify scintillation close to the RISR-C field-aligned beam, the ionospheric pierce points (IPPs) that corresponded to an elevation angle higher than 40 degrees were used.
- Other complementary data from AMPERE, SuperDARN, solar wind monitor are also used to assist the interpretation of the scintillation events that were investigated.

3) Statistical Analysis

Patch Scintillation Distribution

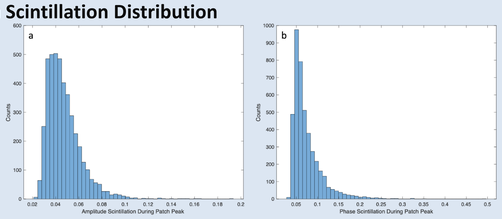

Figure 1: Histograms of the distribution of amplitude (a) and phase (b) scintillations during the peak of a polar cap patch.

- Figure 1 displays the distributions of amplitude (a) and phase (b) scintillations during the peak of polar cap patches.
- The majority of scintillations fall below 0.06 (more than 80%) for the amplitude S4 index and 0.1 (more than 80%) for phase.
- There were 33 enhanced scintillation events for the phase scintillation ($\sigma_\Phi > 0.2$). Of those 33 events, 4 had $\sigma_\Phi > 0.3$, and 1 event had $\sigma_\Phi > 0.4$.
- For the amplitude scintillation, there were no events with an amplitude scintillation index over 0.2.
- However, 21 patches had S4 > 0.1, and 4 out of the 21 patches had S4 > 0.15.
- The distributions of the patch edges are similar to the peak distribution for both the amplitude and phase scintillation.

Patch Center

- Figure 2 shows the amplitude (a) and phase (b) scintillation differences between the daily average and the 3-minute patch average. 79.5%(83.11%) of the absolute differences shown in panel a (b) lie between 0.01 (0.03), indicating that **the amplitude or phase scintillations (a) in those patch events are not significantly different from the daily averages.**
- Similar results were found for the patch edges. The distribution is asymmetric with a longer tail on the negative value side, which indicates that the phase scintillation within patches indeed increased in 55 events (difference < -0.03). For the amplitude scintillation, the same is true where the scintillation increased for 68 events (difference < -0.01).

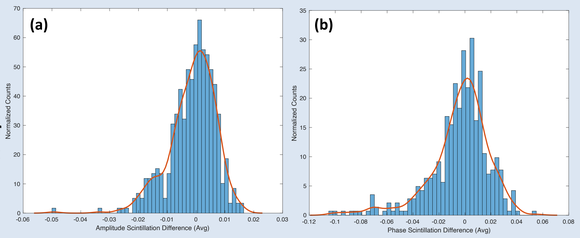

Figure 2: Histogram and kernel density curve of the amplitude (a) and phase scintillation (b) difference between the daily average and the 3-minute patch average.

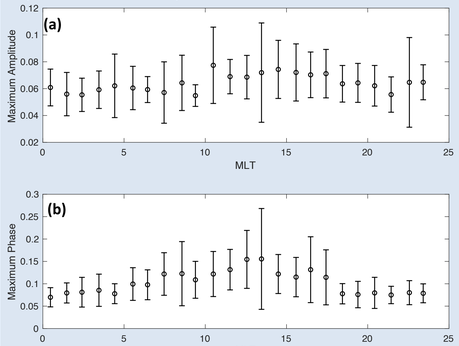

Figure 3: The average of each MLT hour of the maximum amplitude (a) and phase (b) scintillation that occurred in a 3-minute period centered on when a patch was observed.

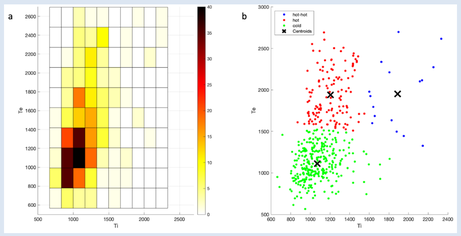

Figure 4: (a) Mosaic plot of the ion and electron temperatures associated with polar cap patches (b) classifications of the patches by ion and electron temperatures divided into three categories: hot, hot-hot, and cold

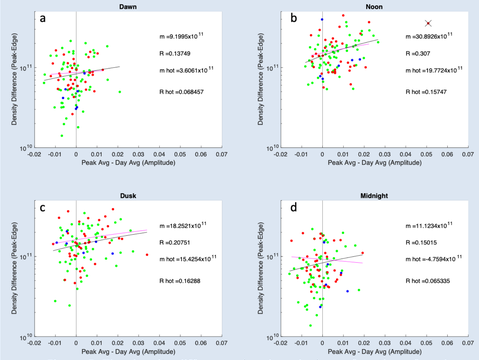

Figure 5: The density difference (peak - edge) as a function of peak average minus daily average amplitude scintillation for different MLT time periods

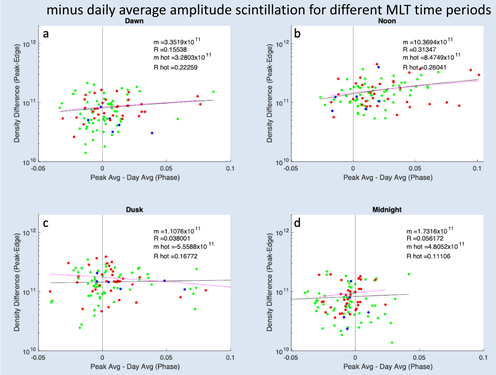

Figure 6: The density difference (peak - edge) as a function of peak average minus daily average phase scintillation for different MLT time periods

MLT Dependence

- Figure 3 shows a clear relationship between MLT and maximum amplitude and phase scintillations during polar cap patches.
- For each MLT hour, the average was taken of the maximum scintillation within a 3-min window at patch center as shown by (a) with amplitude scintillation and (b) with phase scintillation.
- **The phase scintillation (3b) is higher near noon MLT than that at other MLTs.** This relationship is not as clearly visible in the amplitude scintillation in Figure 3(a).
- Of the 55 events where significant phase scintillation was observed, 56.4% occurred during noon MLT (09-15 MLT), 14.5% occurred during dawn MLT (03-09 MLT), 25.5% occurred during dusk MLT (15-21 MLT), and less than 1% occurred during midnight MLT (21-03 MLT).
- Of the 68 events where significant amplitude scintillation was observed, 45.6% occurred during noon MLT, 7.4% occurred during dawn MLT, 39.7% occurred during dusk MLT, and 7.4% occurred during midnight MLT.

Patch Temperature Dependence

- Figure 4 (a) shows the distribution of Te and Ti associated with patches in a 2D mosaic plot.
- One can see that the majority of the patches are below 1400 K for Te and 1400 K for Ti, which would belong to the cold patch class as defined in Figure 4 (b).
- To define a hot or cold patch, we used a classification algorithm provided by MATLAB called kmeans, which uses Lloyd's algorithm.
- Figure 4 (b) shows three different patch temperature classifications, including cold (Ti ~=Te and Te <~1500 K), hot (Te >> Ti and Te >~1500 K), and hot-hot (Ti~=Te and Ti >~1500 K).
- Figure 5 shows the distribution of hot (red), cold (green), and hot-hot (blue) patches in the same color scheme as Figure 4 for different MLT sectors as labeled. The y axis is the difference between the peak and edge density, in order to view any trend in the density gradient of the patches. The x axis is the difference between the peak average and the day average amplitude scintillation, positive indicating enhanced patch scintillation.
- The black lines show the linear fit of all of the patches within the sector, while the magenta line shows the linear fit of just the hot patches within the sector.
- The noon (b) and dusk (c) sectors show more patches on the positive side indicating that patches that occur during noon and dusk have higher amplitude scintillation than the other two sectors.
- Figure 6 is in the same format as Figure 5, but for phase scintillation.
- **In both figures, the largest correlation and the largest slope are shown in (b) at noon time for all patches within the same sector. This correlation coefficient is > 0.3, which is moderately significant.**
- **These findings suggest that the larger the patch density gradients, the higher the scintillation levels.**
- **This relationship for the hot patch class is similar to the overall trend.**

4) Event Analysis

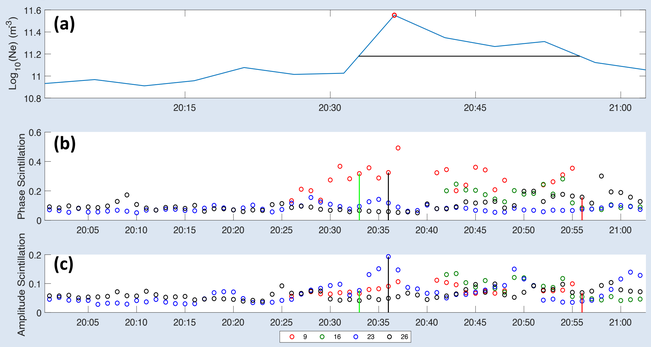

Figure 7: (a) Electron Density, (b) Phase, and (c) Amplitude scintillation from several PRNs. In(a), the patch width is shown marked with a black horizontal line at 75% prominence with the red star marking the patch center. The green line marks the leading edge, the black line marks the center, and the red line marks the trailing edge in (b) and (c).

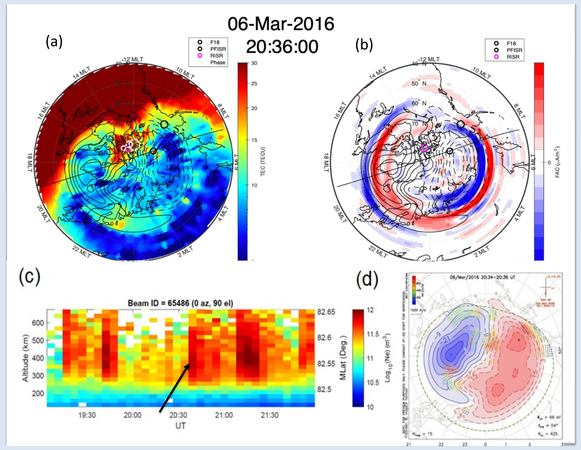

Figure 8: (a) Total Electron Content Map showing in units of TECU (b) Current density at March 6, 2016 at 20:35 UT. The phase scintillations observed are also plotted as black circles (c) The electron density from RISR on March 06, 2016 between 19 UT and 22 UT (d) Ionosphere convection map for March 6, 2016 between 20:34 and 20:36 UT. Figure from SuperDARN Virginia Tech.

- One example of increased scintillation with patch presence occurred on March 6, 2016, between 20:00 and 21:00 UT, when the phase scintillation increased to greater than 0.4 radians at the center of the patch as shown by PRN 9 in Figure 7 (b). Figure 7 (c) shows the amplitude scintillation also increased slightly, ~0.2 for the center of the patch, as shown by PRN 23.
- The dayside TEC increased around 20:35 UT as shown by Figure 8 (a), i.e., storm-enhanced density (SED), and the SED plume extended poleward into the polar cap forming patches. Interestingly, the Resolute Bay receiver was just poleward of the cusp near the noon MLT.
- The maximum phase scintillation occurred at 20:37 UT, which coincides with the sharp density gradient there in Figure 8(c). Figure 8(d) shows that the convection flow speed was very high (~800 m/s) in the region where the patch was observed.
- It is likely that polar cap patches that are severe enough with large electron density and sharp density gradient, as well as large convection flows to enhance scintillation significantly.
- The detailed instability mechanism is under investigation.

5) Conclusion

- Comparing the 3-minute averaged scintillation when a patch occurred to the scintillation averaged over one day, it was noted that ~80% of the patches do not show a significant scintillation level increase.
- There is no significant scintillation differences between the patch center and edges at Resolute Bay.
- However, around 15% of patches are associated with enhanced scintillations. Of those patches, a majority occurred during noon MLT.
- Within the noon sector, the larger the patch density gradients, the higher the scintillation levels.
- We have classified patches into different categories based on plasma temperature and did not find clear scintillation level dependence among the different categories.
- A patch itself may not be a sufficient condition for the scintillation to increase. It may cause scintillation if paired with other effects, such as sharp density gradient and fast convection flow. More quantitative work is needed to find out the exact instability mechanisms for patch to enhance scintillation.

For further questions, please contact alanahco@umich.edu at the University of Michigan

Acknowledgements

The scintillation data was provided by CHAIN (http://chain.physics.unb.ca/chain/pages/gps/). The solar wind data was provided by NASA OMNIWeb service (http://omniweb.gsfc.nasa.gov). The field-aligned current data was provided by AMPERE (http://ampere.jhuapl.edu/products/plots/). The convection map were provided by SuperDARN (http://vt.superdarn.org/tiki-index.php?page=Conv+map+overview). AC was supported by funding provided by the Michigan Space Grant Consortium (MSGC), and NASA 80NSSC20K1313. SZ and JR are supported by NASA 80NSSC20K1313 and 80NSSC20K0600.

References

Hapgood, M. (2017), Jenner, L. A. et al. (2020), Kintner, P. M et al.(2007), Knepp, D. L. (2015), Matsui, H. et al.(2017), Oksavik, K. et al.(2015), Prikryl, P., Jayachandran et al. (2012), Ren, J. et al.(2018), Strangeways, H. J. (2009), van der Meeren, C., et al.(2014), Wang, Y., et al. (2018), Hosokawa, K., et al. (2009), Coley, W. R., & Heelis, R. A. (1995)